Study on the Stability and Motion Control of a Unicycle*
(Part I: Dynamics of a Human Riding a Unicycle and Its Modeling by Link Mechanisms)

Zaiquan SHENG** and Kazuo YAMAFUJI**

In this paper, the dynamic characteristics of a human riding a unicycle are analyzed following observation. From the observation and analysis, we found that the rider's trunk, thighs and shanks form two closed-link loops, and this special mechanism plays an important role in the stability of the unicycle. Based on this idea, we developed a new model with two closed-link mechanisms and one turntable to enable a robot to emulate a human riding a unicycle. Considering the nonholonomic constraint between the wheel and ground, and using a recently developed general method to compute the multi-closed-link mechanisms' dynamic motion, we obtained the dynamic equations of motion for this new model. With these equations, the simulation is conducted under the proposed control method. The simulation result indicates that both the longitudinal and lateral stability of a unicycle ridden by a human can be satisfactorily emulated by this new model.

Key Words: Nonlinear System, Two Closed-Link Loops, Nonholonomic Constraint Dynamics, Longitudinal and Lateral Stability, Modeling

1. Introduction

One of the important fields in research on robotics is the emulation of the intelligence or capabilities which are inherited by human beings or animals. As to locomotive capability, it is clear that human beings and some animals have quite excellent locomotion in walking, running or jumping. We believe that it will be beneficial to emulate human and animal walking, running and jumping by robot. In fact, in recent years results have been reported by some researchers[1]-[3] who attempted this.

Our attention is focused on emulating human riding of a unicycle by robot. We know that a person uses not only his flexible body and good sensory systems, but also his skill and computational abilities to stabilize the unicycle; meanwhile its speed and direction can also be controlled. To do research on this problem, the following questions should be answered.

1. In what way does a person stabilize the unicycle and control its direction and speed?
2. What kind of practical mechanical model is necessary and suitable for us to emulate human riding of a unicycle by a robot? This means determining how many degrees of freedom are needed and how many actuators are necessary. Of course, the model should also be practical enough to be manufactured.
3. What kinds of sensors will be suitable and practical for use in the control of the robot?
4. Because the unicycle problem is an inherently unstable problem, what kind of control method will be suitable for it?
5. Does the robot emulator have better stability than a human riding a unicycle or not?

As stated above, the process of a human riding a unicycle is quite complex, and the many unanswered questions in the system make the unicycle problem interesting. Actually, the unicycle problem has previously attracted the attention of some researchers. Feng and Yamafuji[4] investigated the unicycle problem, using an inverted pendulum with a controlling arm pivoted at its upperend, in 1985, and similar

* Received 1st November, 1993.
** Department of Mechanical and Control Engineering, University of Electro-Communications, 1-5-1 Chofugaoka, Chofu, Tokyo 182, Japan

research was also conducted by Yamafuji and Inoue[5]. Although this research was successful both in terms of simulation and experimentation, the investigation dealt only with the two-dimensional problem of the unicycle. Schoonwinkel[6] conducted research by modeling a human riding a unicycle with three rigid bodies, which were a wheel, a frame representing the unicycle frame and lower part of the rider's body, and a rotary turntable to represent the rider's twisting torso and arms. His research is mainly concentrated on the robot's construction and on the evaluation of balance sensors, but no good experimental result was reported. Vos and von Flotow[7] used Schoonwinkel's model and carried out research. Their work proposes a new LQG structure for the control and mainly deals with the nonlinear problem of dry friction between the wheel and floor in the yaw direction. Some experimental results are reported in their paper[7], but none on roll angle or roll angular velocity. In fact, the yaw rate and the rotary turntable rate are not always so low that the lateral and longitudinal dynamics can nominally be decoupled. Furthermore, they have not dealt with the nonlinearly coupled problem between lateral and longitudinal dynamics due to large yaw rate and yaw accelerations.

In this paper, based on the analysis of the unicycle problem by the observation of a human riding a unicycle, we propose a new model to emulate the human riding a unicycle. In this model there is a wheel, two closed-link mechanisms to represent the rider's body, thighs, and shanks, and pedals on the unicycle. Meanwhile, a rotary turntable represents the rider's twisting torso and arms as in Schoonwinkel's model. With this new model and considering the nonholonomic constraints between the wheel and ground, we derive the dynamic equations of motion. By using these newly developed equations of motion to control the system, the result of computer simulation was obtained. The simulation results indicate that this model is adequate and successful in obtaining stability and well represents the practical case of a human riding a unicycle.

2. Observation of Human Riding a Unicycle and Its Stability Principle

The process of a human riding a unicycle is quite complex. The model of a human riding a unicycle is simply shown in Figure 1. Based on the observation of an experienced human riding a unicycle, we can summarize the characteristics of this process as follows:

1. A person uses a large amount of information on sensory inputs to monitor the process, and the control actions themselves are nonlinear. As is the case with most skills learned by a human rider, many of the feedback control loops are closed at a subconcious level.

2. A person on a unicycle maintains longitudinal stability by pedaling faster or slower with one side of thighs and shanks, by leaning his torso forward or backward and by moving his arms forward and backward; the two sides of thighs and shanks are used alternately, not simultaneously. Torso and arm movements provide recovery force for longitudinal stability, but the recovery force provided is limited, so the rider has to pedal the wheel faster or slower for longitudinal stability. Lateral stability is obtained by leaning his torso sideways, pulling an arm in or stretching it out, and by steering the wheel into the direction in which he is falling by twisting motions at the hip joints. The lateral and longitudinal stabilities are highly coupled together, and usually the lateral stability is realized by turning the unicycle into the direction in which he is falling and then using the longitudinal control system to vertically correct the unicycle. Both longitudinal and lateral control systems are important, but the longitudinal one seems more important.

3. Many of the control actions are rather jerky. For example, when a person wants to change direction on a unicycle, he uses his torso and outstretched arms for reaction inertia to suddenly twist the part of his body and the unicycle in the desired direction. He uses his knowledge (gained by experience) of the nonlinear friction characteristics of the wheel on the ground to apply a correct torque profile to end up in the desired direction. Simultaneously, the rider leans into the turn to counteract the effect of the ground reaction force and the inertia of his body, which tends to make the rider fall towards the direction in which he has been travelling.

To emulate the above-described process of a human riding a unicycle by a robot would be so prohibitively complex that it would not be practical enough to be simulated and implemented in a laboratory. Thus, it is better for us to gain insight into the processes involved, and grasp the fundamental and important aspects to construct a simple but practical and active robot to emulate this complex process.

From the observation of experienced unicycle riders' demonstrations, we know that a person on a unicycle maintains longitudinal stability mainly by pedaling faster or slower; the leaning of his torso forward or backward is performed, but within a small range, and the movement of his arms forward and backward is not in a large range, either. On the other hand, we find that the rider's body, thighs, and shanks, and the pedals on the unicycle can form two closed-link mechanisms, as shown in Fig. 1. Because the

rider takes advantage of this special structure, he can maintain longitudinal stability at the desired speed. If the unicycle is held by a person who is not the rider, the rider can use the two pedals on the unicycle to maintain his body's longitudinal stability easily. However, if there are not any pedals on the unicycle for the rider to use, we can easily imagine that the rider will not be able to maintain the longitudinal stability of his body on the fixed unicycle no matter how hard he tries. From this observation and analysis, it is reasonable for us to assume that the pedals and the special closed-link mechanisms formed by the rider's body, thighs, and shanks with pedals play an important role in the process of a human riding a unicycle. Therefore, we propose to use two closed-link mechanisms to represent the rider's body, thighs, shanks and pedals on a unicycle, and with these two closed mechanisms, emulate the rider's actions of pedaling faster or slower, leaning his torso forward or backward, and moving his arms forward or backward.

Observation of an experienced human riding a unicycle shows that lateral stability is obtained largely by continuously twisting the wheel in order to steer towards the direction that he is falling. A turntable mounted on the top of the robot with its axis of rotation along the centerline of the unicycle is proposed to simulate the rider's torso and arms.

Based on the above proposed idea, we can obtain a mechanical link model as drawn in Fig. 2, in which there is a wheel, and two closed-link mechanisms to represent the rider's body, thighs, shanks and pedals on a unicycle; meanwhile, a rotary turntable is used to represent the rider's twisting torso and arms as in Schoonwinkel's model. As shown in Fig. 2, link 1, link 2, right pedal and body form a five-bar closed-link mechanism. Link 3, link 4, left pedal and body form another five-bar closed-link mechanism. Meanwhile, these two closed-link mechanisms have the body as a common part, and the right pedal has the same axis as the left pedal. The structure with two closed-link mechanisms has only two degrees of freedom. One is this structure's rotation around support axis y_1y_2 in the pitch direction; another is the wheel's rotation around axis y_1y_2 in the pitch direction. In the process of a human riding a unicycle, the wheel is driven through applying force at joint 1, joint 2 or joint 3, as shown in Fig. 1. If the robot is designed to operate in such a manner, it will be quite complicated, and so many motors will be needed. In the design of a robot, to realize the same goal, it is better to use fewer motors.

In this structure, PATTERN 1 and PATTERN 2 are available for driving the mechanisms. PATTERN 1 uses only two motors for driving link 1 or link 3 at joint A 1 or A 2; with this pattern the wheel is driven and the longitudinal stability is also obtained by these two motors. This pattern is quite similar to the human-riding-unicycle system in which one side of the thighs and shanks is used to pedal the unicycle; the analysis in the following sections will show whether this pattern is suitable or not. PATTERN 2 uses three motors, one for driving the wheel, the other two to drive link 2 or link 4 at joint C or joint F, to maintain longitudinal stability. In fact, as analyzed above, since the structure with two closed-link mechanisms has only two degrees of freedom, two actuators are sufficient for its control. One motor for the wheel and another motor for link 2 or link 4 are sufficient for this structure. If three motors are used in this pattern,

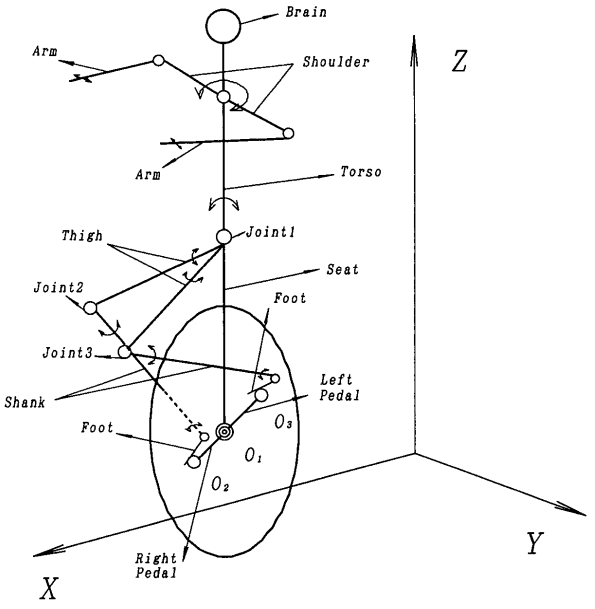

Fig. 1 Schematic diagram of human riding unicycle

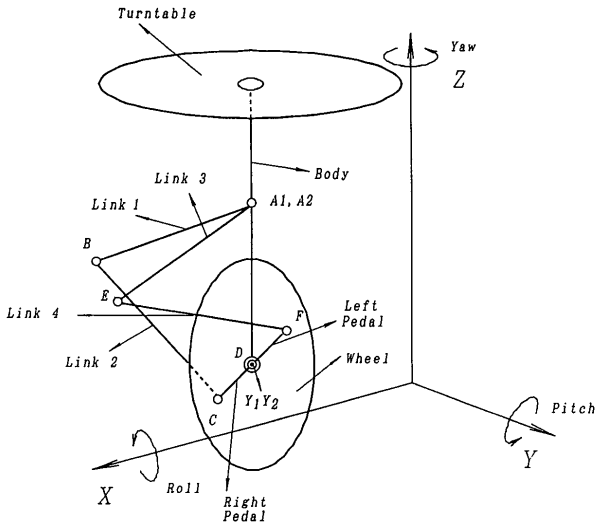

Fig. 2 Robot model emulating human riding unicycle

PATTERN 2 will be a redundant system. We have performed the analysis when PATTERN 2 is driven by two or three motors, and found that the analysis results are similar; the only difference lies in the requirement of the motor's driving torque. On the other hand, considering the structure's symmetry and balance, we recognized that the pattern with three motors will be more practical than the pattern with two motors, and it is easier for us to design the unicycle robot using the pattern with three motors. For the above reasons, in PATTERN 2 we propose to use two motors to drive link 2 and link 4, with the torques for those two motors taken as the same to consider the effect of the structure's redundancy, and use one motor to drive the wheel directly. In order to make the paper concise and explicit, we introduce only the analytical result on PATTERN 2 with three motors for driving the wheel and for maintaining longitudinal stability in this paper.

From the analysis in the following sections, we know that PATTERN 2 is more practical than PATTERN 1. In the design of a robot, taking into account balance and symmetry of the structure, link 1 will be designed the same as link 3; similarly link 2 will also be the same as link 4.

A person uses several sensory systems to monitor the stabilization process while riding a unicycle. The four major sensors used to determine orientation with respect to the vertical are the vestibular system, visual system, proprioceptive sensors and tactile sensors[7]-[9]. The vestibular system is the primary orientation system of the human and consists of the semicircular canals (which responds to angular velocity of the head) and the otolith organs (which respond to linear acceleration and to changes in orientation with respect to the gravity vector). Proprioceptive cues are obtained from limb position signals and muscle length and tension afferents, from which the brain can infer which dynamic forces are acting on the body, based on the person's experience on coordination. A person can also determine his orientation with respect to the vertical from tactile pressure cues on the various parts of his body which are in contact with his environment. Finally eyesight is used in combination with a person's experience in deducing the direction of the vertical from clues in his environment, to give an indication of his lateral and longitudinal orientation. All these sensory inputs are combined in the human brain to determine the spatial orientation of his body. It is obviously impossible to obtain robot sensors with all the sophistication mentioned above. We shall first use basic distance and rate sensors to perform the experiment. If these sensors are not adequate, we plan to use acceleration sensors and other more accurate sensors in our experiments.

3. Modeling of the Dynamic System

To test whether the proposed model is appropriate for emulating a human riding a unicycle or not, we first have to analyze the mechanical dynamic motion of this model. In this model, as shown in Fig. 2, there are two closed-link mechanisms. Thus it is a system with multi-closed link mechanisms, and we must have a method to compute the dynamic motion for it. There was no practical method available until we developed an effective method which is reported in another paper[10]. We shall apply this method to the computation of this model as follows after we define the coordinates, consider the friction in the system as linear viscous friction and assume there is no slip between the wheel and ground.

In Fig. 3, we present the link model of the proposed model and parameters that will be used in our computation. The calculation of the displacement of every part's gravity center relative to the world reference coordinate $x_r y_r z_r$ in the model is performed according to the coordinates defined in Fig. 4. In Fig. 4, $x_r y_r z_r$ is the world reference coordinate, $x_0 y_0 z_0$ is obtained by translating $x_r y_r z_r$ through vector $(x_0, y_0, 0)$; rotate $x_0 y_0 z_0$ along z_0 by α, then obtain $x_1 y_1 z_0$; rotate $x_1 y_1 z_0$ along x_1 by γ, then obtain $x_1 y_2 z_2$; $x_3 y_3 z_3$ is obtained by translating $x_1 y_2 z_2$ through vector $(0, 0, \gamma_w)$; $x_4 y_4 z_4$ is obtained by rotating $x_3 y_3 z_3$ along y_3 by ψ and then translating it by vector $(e_3, 0, 0)$; $x_5 y_5 z_5$ is obtained by rotating $x_3 y_3 z_3$ along y_3 by ψ and then translating it by vector $(-e_3, 0, 0)$; $x_6 y_6 z_6$ is obtained by rotating $x_3 y_3 z_3$ along y_3 by β and then translating it by vector $(0, 0, e_5)$; $x_7 y_7 z_7$ is obtained by rotating

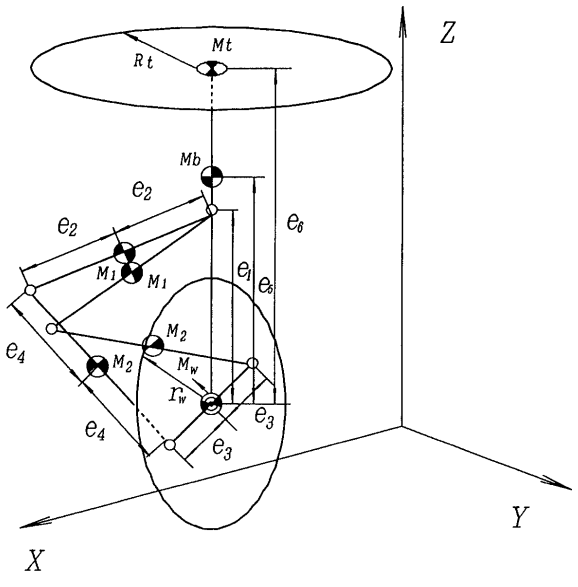

Fig. 3 Link model and its parameters for simulation

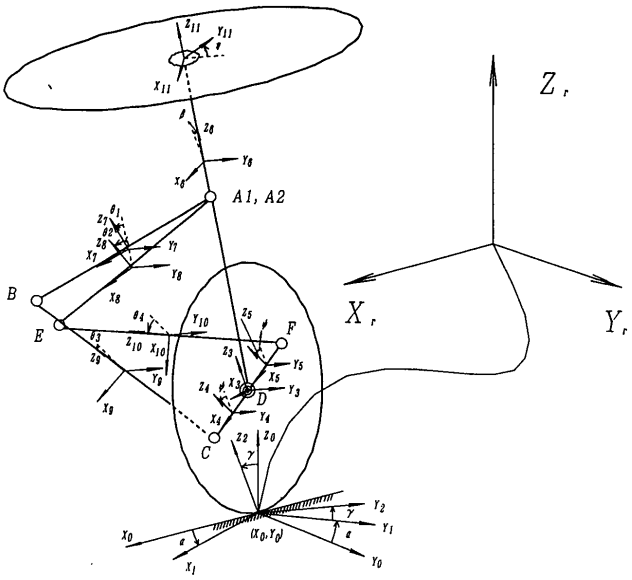

Fig. 4 Illustration of coordinates

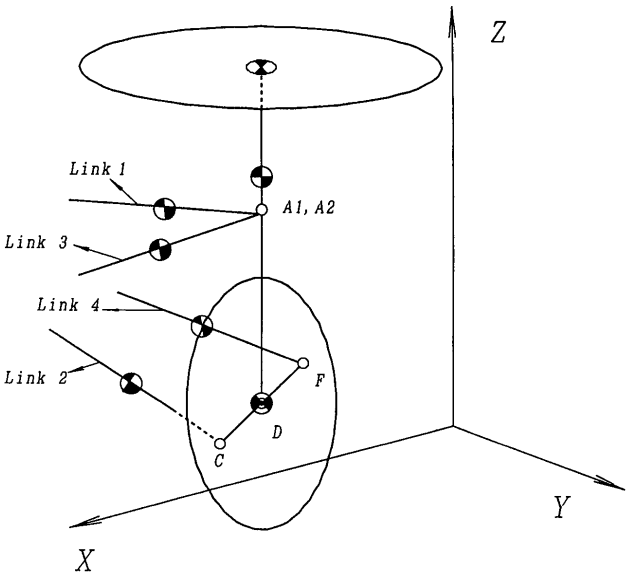

Fig. 5 Equivalent open-tree-structure link mechanism of the model

$x_6y_6z_6$ along y_6 by θ_1 and then translating it by vector $(e_2, 0, e_1-e_5)$; $x_8y_8z_8$ is obtained by rotating $x_6y_6z_6$ along y_6 by θ_3 and then translating it by vector $(e_2, 0, e_1-e_5)$; $x_9y_9z_9$ is obtained by rotating $x_4y_4z_4$ along y_4 by θ_2 and then translating it by vector $(0, 0, e_4)$; $x_{10}y_{10}z_{10}$ is obtained by rotating $x_5y_5z_5$ along y_5 by θ_4 and then translating it by vector $(0, 0, e_4)$; and $x_{11}y_{11}z_{11}$ is obtained by rotating $x_6y_6z_6$ along z_6 by η and then translating it by vector $(0, 0, e_6-e_5)$.

Assume there is rolling motion between wheel and ground and no slip between them; this implies

$$\dot{x}_0=\gamma_\omega\dot{\psi}\cos\alpha \quad (1)$$

$$\dot{y}_0=\gamma_\omega\dot{\psi}\sin\alpha \quad (2)$$

The unicycle's motion is constrained by the above two nonholonomic constaint equations. In the computation, all the friction is assumed to be linear viscous friction in order to make the analysis simple; then the dynamic computation for this model is developed in the following five steps.

Step 1: In the closed-link mechanism A 1 BCD, select joint B which is not driven by an independent actuator. Assume that joint B is cut open so that the closed-link mechanism becomes an open-link mechanism in a tree structure with three joints A 1, C and D. Each joint in the open-link mechanism is to be driven virtually by an actuator to yield one degree of freedom. Similarly, in the closed-link mechanism A 2 EFD, select joint E which is not driven by an independent actuator. Assume that joint E is cut open so that the closed-link mechanism becomes an open-link mechanism in a tree structure with three joints, A 2, F and D. Each joint in the open-link mechanism is to be driven virtually by an actuator to yield one degree of freedom, also. The unicycle's mechanism with two open-link tree structures is shown in Fig. 5. As shown in Fig. 5, there are nine degrees of freedom in this open-link tree structure mechanism; they are ψ, α, γ, β, η, θ_1, θ_2, θ_3 and θ_4.

Step 2: The four constraint equations due to two closed-link loops are calculated as the following four equations;

$$e_1\sin\beta+2e_2\cos(\theta_1+\beta)-e_3\cos\psi-2e_4\sin(\psi+\theta_2)=0 \quad (3)$$

$$e_1\cos\beta-2e_2\sin(\theta_1+\beta)+e_3\sin\psi-2e_4\cos(\psi+\theta_2)=0 \quad (4)$$

$$e_1\sin\beta+2e_2\cos(\theta_3+\beta)+e_3\cos\psi-2e_4\sin(\psi+\theta_4)=0 \quad (5)$$

$$e_1\cos\beta-2e_2\sin(\theta_3+\beta)-e_3\sin\psi-2e_4\cos(\psi+\theta_4)=0 \quad (6)$$

Differentiating the above constraint equations two times with respect to time, we obtain the following constaint equations on acceleration.

$$\begin{aligned}&(e_3\sin\psi-2e_4\cos(\theta_2+\psi))\ddot{\psi}+(e_1\cos\beta-2e_2\sin(\theta_1+\beta))\ddot{\beta}-2e_2\sin(\theta_1+\beta)\ddot{\theta}_1\\&-2e_4\cos(\theta_2+\psi)\ddot{\theta}_2-(e_1\sin\beta+2e_2\cos(\theta_1+\beta))\dot{\beta}^2-2e_2\cos(\theta_1+\beta)\dot{\theta}_1^2\\&+(e_3\cos\psi+2e_4\sin(\theta_2+\psi))\dot{\psi}^2+2e_4\sin(\theta_2+\psi)\dot{\theta}_2^2+4e_4\sin(\theta_2+\psi)\dot{\psi}\dot{\theta}_2\\&-4e_2\cos(\theta_1+\beta)\dot{\beta}\dot{\theta}_1=0\end{aligned} \quad (7)$$

$$\begin{aligned}&(e_3\cos\psi+2e_4\sin(\theta_2+\psi))\ddot{\psi}-(e_1\sin\beta+2e_2\cos(\theta_1+\beta))\ddot{\beta}-2e_2\cos(\theta_1+\beta)\ddot{\theta}_1\\&+2e_4\sin(\theta_2+\psi)\ddot{\theta}_2-(e_3\sin\psi-2e_4\cos(\theta_2+\psi))\dot{\psi}^2-(e_1\cos\beta-2e_2\sin(\theta_1+\beta))\dot{\beta}^2+2e_2\sin(\theta_1+\beta)\dot{\theta}_1^2\\&+2e_4\cos(\theta_2+\psi)\dot{\theta}_2^2+4e_2\sin(\theta_1+\beta)\dot{\beta}\dot{\theta}_1+4e_4\cos(\theta_2+\psi)\dot{\psi}\dot{\theta}_2=0\end{aligned} \quad (8)$$

$$-(e_3\sin\psi+2e_4\cos(\theta_4+\psi))\ddot{\psi}+(e_1\cos\beta$$

$$-2e_2\sin(\theta_3+\beta))\ddot{\beta}-2e_2\sin(\theta_3+\beta)\ddot{\theta}_3$$
$$-2e_4\cos(\theta_4+\psi)\ddot{\theta}_4-(e_3\cos\psi$$
$$-2e_4\sin(\theta_4+\psi))\dot{\psi}^2-(e_1\sin\beta$$
$$+2e_2\cos(\theta_3+\beta))\dot{\beta}^2-2e_2\cos(\theta_3+\beta)\dot{\theta}_3^2$$
$$+2e_4\sin(\theta_4+\psi)\dot{\theta}_4^2+4e_4\sin(\theta_4+\psi)\dot{\psi}\dot{\theta}_4$$
$$-4e_2\cos(\theta_3+\beta)\dot{\beta}\dot{\theta}_3=0 \quad (9)$$

$$(-e_3\cos\psi+2e_4\sin(\theta_4+\psi))\ddot{\psi}-(e_1\sin\beta$$
$$+2e_2\cos(\theta_3+\beta))\ddot{\beta}-2e_2\cos(\theta_3+\beta)\ddot{\theta}_3$$
$$+2e_4\sin(\theta_4+\psi)\ddot{\theta}_4+(e_3\sin\psi$$
$$+2e_4\cos(\theta_4+\psi))\dot{\psi}^2-(e_1\cos\beta$$
$$-2e_2\sin(\theta_3+\beta))\dot{\beta}^2+2e_2\sin(\theta_3+\beta)\dot{\theta}_3^2$$
$$+2e_4\cos(\theta_4+\psi)\dot{\theta}_4^2+4e_2\sin(\theta_3+\beta)\dot{\beta}\dot{\theta}_3$$
$$+4e_4\cos(\theta_4+\psi)\dot{\psi}\dot{\theta}_4=0 \quad (10)$$

Step 3: By use of the coordinates defined in Fig. 4, we can calculate the translational kinetic energy, rotational kinetic energy and potential energy for wheel, body, links and turntable, and using this calculated mechanical energy, we can compute the equations of motion for all the joints using Lagrange's method for the virtual open-link mechanism shown in Fig. 5. Because there are two nonholonomic constraint equations (1) and (2) to constrain the unicycle's motion, as pointed out in Rosenberg[11], Lagrange's equation for a system with n generalized coordinates, q_i, and k nonholonomic constraint equations, ξ_j, should be

$$\frac{d}{dt}\left(\frac{\partial L}{\partial \dot{q}_i}\right)-\frac{\partial L}{\partial q_i}=\sum_{j=1}^{k}\mu_j\delta_{ji}+\theta_i \quad (\text{for } i=1, 2, \cdots, n), \quad (11)$$

where Q_i are the generalized forces which are not derivable from a potential function (the applied torques from the motors and friction in this case), and

$$\delta_{ji}\equiv\frac{\partial\xi_j}{\partial q_i}, \quad (12)$$

where ξ_j are the constraint equations of the system.

In this virtual open-link mechanism, the generalized coordinates q_i are $(x_0, y_0, \psi, \alpha, \gamma, \beta, \theta_1, \theta_2, \theta_3, \theta_4, \eta)$ and the nonholonomic constraint equations ξ_i are Eqs. (1) and (2). After the dynamic equations of motion are derived with the above Lagrange method, eliminate coordinates x_0 and y_0 by substituting the following equations into the dynamic equations of motion obtained. Then the dynamic equations of motion for the virtual open-link mechanism can be described by Eq. (17).

$$\dot{x}_0=\gamma_\omega\dot{\psi}\cos\alpha \quad (13)$$
$$\dot{y}_0=\gamma_\omega\dot{\psi}\sin\alpha \quad (14)$$
$$\ddot{x}_0=\gamma_\omega(\ddot{\psi}\cos\alpha-\dot{\psi}\dot{\alpha}\sin\alpha) \quad (15)$$
$$\ddot{y}_0=\gamma_\omega(\ddot{\psi}\sin\alpha+\dot{\psi}\dot{\alpha}\cos\alpha) \quad (16)$$
$$\tau=M(q)\ddot{q}+B(q)[\dot{q}\dot{q}]+C(q)[\dot{q}^2]+D(q)[\dot{q}]+G(q) \quad (17)$$

$\tau=(\tau_\psi, \tau_\alpha, \tau_\gamma, \tau_\beta, \tau_{\theta_1}, \tau_{\theta_2}, \tau_{\theta_3}, \tau_{\theta_4}, \tau_\eta)^T$ is the torque matrix for the virtual open-link mechanism; $M(q)$ is a 9×9 matrix of mass; $B(q)$ is a matrix of dimensions 9×36 of Coriolis coefficients, $[\dot{q}\dot{q}]$ is a 36×1 vector of velocity products given by $[\dot{q}\dot{q}]=[\dot{\psi}\dot{\alpha}\ \dot{\psi}\dot{\gamma}\ \cdots\ \dot{\theta}_4\dot{\eta}]^T$; $C(q)$ is a 9×9 matrix of centrifugal coefficients, and $[\dot{q}^2]$ is a 9×1 vector given by $(\dot{\psi}^2, \dot{\alpha}^2, \dot{\gamma}^2, \dot{\beta}^2, \dot{\theta}_1^2, \dot{\theta}_2^2, \dot{\theta}_3^2, \dot{\theta}_4^2, \dot{\eta}^2)^T$; $D(q)$ is a 9×9 matrix of friction coefficients and $[\dot{q}]=(\dot{\psi}, \dot{\alpha}, \dot{\gamma}, \dot{\beta}, \dot{\theta}_1, \dot{\theta}_2, \dot{\theta}_3, \dot{\theta}_4, \dot{\eta})^T$; $G(q)$ is a 9×1 matrix of gravity terms. Here q is defined as a matrix $(\psi, \alpha, \gamma, \beta, \theta_1, \theta_2, \theta_3, \theta_4, \eta)^T$.

Step 4: Consider the constraints presented in Eqs. (3)~(6) and compute the original closed mechanism motion, following Eq. (18). Because the coordinates that are not included in the closed-link loop do not contribute to the constraints for closed-link loops, the calculation of the dynamic motion for open-link coordinates α, γ and η is the same as computed in Eq. (17); only the calculation of coordinates ψ, β, θ_1, θ_2, θ_3 and θ_4, which belong to the closed-link loops, is performed using

$$\tau+\left(\frac{\partial c}{\partial q}\right)\lambda=M(q)\ddot{q}+B(q)[\dot{q}\dot{q}]+C(q)[\dot{q}^2]+D(q)[\dot{q}]+G(q), \quad (18)$$

where $\frac{\partial c}{\partial q}$ is a 4×4 matrix determined by constraint equations (3)~(6). λ is a 4-dimensional vector of Lagrangian multipliers. The other symbols in Eq. (18) are the same as in Eq. (17), but they only indicate the members that belong to the dynamic equations of motion for the coordinates included in closed-link loops.

In PATTERN 1, set $\tau_\psi=0$, $\tau_\beta=0$, $\tau_{\theta_2}=0$ and $\tau_{\theta_4}=0$, which are not driven by independent actuators. In PATTERN 2, set $\tau_\beta=0$, $\tau_{\theta_1}=0$ and $\tau_{\theta_3}=0$, which are not driven by independent actuators. Meanwhile, the open-link coordinates α and γ are also not driven by independent actuators; thus τ_α and τ_γ are also set to zero.

Step 5: Rearrange the equations using constraint equations on the closed-link loop acceleration, Eqs. (7)~(10) (as in Eq. (9) in Ref. (10)). We can obtain the following Eq. (19), for the computation of the unicycle's dynamic motion, which considers the special structure with two closed-link mechanisms, as well as the nonholonomic constraint due to the rolling between wheel and ground. With this equation, we can compute the unicycle's acceleration, velocity and displacement with the Runge-Kutta-Gill method; then the simulation with generalized input force can be carried out:

where $\tau=(0, 0, 0, 0, \tau_{\theta_1}, 0, \tau_{\theta_3}, 0, \tau_\eta)$ in PATTERN 1 or $\tau=(\tau_4, 0, 0, 0, 0, \tau_{\theta_2}, 0, \tau_{\theta_4}, \tau_\eta)$ in PATTERN 2; $E(q)$ is a 4×4 coefficient matrix for acceleration, $F(q, \dot{q})$ is a 4-dimensional vector for Coriolis and centrifugal terms, and both $E(q)$ and $F(q, \dot{q})$ are determined

from Eqs.(7)~(10); $\frac{\partial C}{\partial q}$ and λ are computed as in Eq.(18). The meanings of other symbols are the same as in Eq.(17).

4. Control algorithms for stability

Since the unicycle's dynamic motion has been developed in section 3, we can input suitable generalized force (it is torque in this case) to the actuators and test whether or not the postural stability of the unicycle can be obtained by simulation at the first stage.

A person drives the unicycle by providing torque to his right and left thighs alternately; in PATTERN 1, the wheel of the emulated unicycle is also driven by inputting torque to the motor that drives link 1 or link 3. Meanwhile, these two motors which drive link 1 or link 3 will also need to contribute to the longitudinal stability. Since we use PATTERN 1 to emulate the functions of the rider's right thigh and left thigh by driving link 1 and link 3 in our model, it is better for us to adopt a control algorithm which is similar to a human riding a unicycle.

From the observation of a human riding a unicycle, we know that in one cycle of the wheel's rotation, half is driven by the rider's right thigh, and another half is driven by the rider's left thigh. The rider always drives the wheel by using left and right thighs alternately. When should the right thigh be used? When should the left thigh be used? It depends on the rider and unicycle's parameters, such as the length of the rider's thigh, the length of the rider's shank and the length of the unicycle's pedal. If the length of the rider's thigh is $2e_2$, the length of the rider's shank is $2e_4$, and the length of the unicycle's pedal is e_3, the same as the length of link 1 (or link 3), link 2 (or link 4) and the length of the unicycle's pedal in our model, then we can draw Fig. 6(a) to show when the right thigh or left thigh should be used (or when link 1 or link 3 should be driven). If one closed-link mechanism is in the state shown in Fig. 6(a) (we shall call it STATE A in the following paragraph), another closed-link mechanism will be in the state shown in Fig. 6(b) (referred to as STATE B in the following paragraph). The configuration shown in Fig. 6(b) is a special configuration for the human-riding-unicycle system or unicycle robot system proposed in our paper; in this special configuration, one of the rider's shanks (link 2 or link 4) coincides with one of the unicycle's pedals. Every closed-link mechanism in our model will change the state between STATE A and STATE B, or exactly at STATE A or STATE B. The change in the closed-link mechanism's state is determined by the wheel's rotation angle in one cycle; we can compute it as $\psi_1=\psi-2\pi\times(\text{int})\frac{\psi}{2\pi}$. If one closed-link mechanism state is changed from STATE A to STATE B, the angle ψ_1 will change from ρ_1 to ρ_2 or from $-\rho_2$ to $-\rho_1$. At the same time, another closed-link mechanism will change its state from STATE B to STATE A. The observation result of the human riding a unicycle tells us that when the side of thighs and shanks is changing from STATE B to STATE A, the thigh at that side will be used to drive the wheel; in the meantime, the thigh on the other side, which is changing from STATE A to STATE B, is not used to drive the system. By the same method, we decide the control algorithm as shown in the

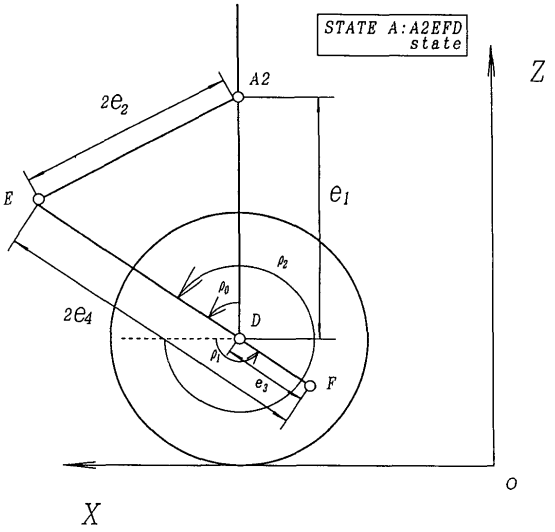

(a) STATE A and parameters used in Eq.(20)

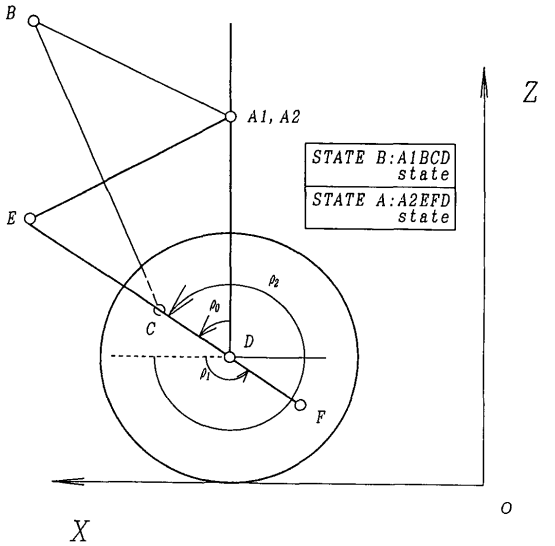

(b) Configuration used to determine the torque to link 1 or link 3

Fig. 6 Geometric position for the change of torque to link 1 or link 3

following, in which link 1 and link 3 are driven alternately, as in a human riding a unicycle.

$$\begin{aligned} &If\ (((\psi_1 \geqslant \rho_1)\ \&\ (\psi_1 < \rho_2))\ \|\ ((\psi_1 \geqslant -\rho_2)\ \&\\ &(\psi_1 < -\rho_1)))\ \text{then}\ \tau_{\theta_1}=0,\\ &\tau_{\theta_3}=A\sin(2\pi\omega t)+kp_1\times\beta+ki_1\times\dot{\beta}\ \text{else}\\ &\tau_{\theta_1}=A\sin(2\pi\omega t)+kp_1\times\beta+ki_1\times\dot{\beta},\ \tau_{\theta_3}=0 \end{aligned} \tag{20}$$

Here

$$\rho_1=\frac{\pi}{2}+\rho_0,\ \rho_2=\frac{3\pi}{2}+\rho_0,\ \rho_0=\arccos\frac{4e_4^2+e_1^2-4e_2^2}{4e_1e_4},$$

$$\psi_1=\psi-2\pi\times(\text{int})\frac{\psi}{2\pi},$$

and ρ_0, ρ_1, ρ_2 are defined and shown in Fig. 6(a); A and ω in Eq.(20) are amplitude and frequency for the driving of the wheel; t is time; and kp_1, ki_1 are feedback gains for longitudinal stability.

In the above control algorithm, $A\sin(2\pi\omega t)$ is used only to represent a common changeable torque to drive the wheel; it does not mean that we must use this kind of torque for the stability control of this system. The parameters like ρ_1, ρ_2, ρ_0 can be easily calculated from the geometric relationship shown in Fig. 6(a).

Lateral stability of the unicycle is realized by applying torque to the motor that drives the turntable to rotate around the central axis of the unicycle's body. As in a human riding a unicycle, the lateral stability must always be obtained as soon as possible. Thus the torque is calculated by the following algorithm. This is a gain schedule method and it is similar to that proposed in research[12] conducted on a one-legged robot which has the controlling rotor on the top of the robot.

$$\tau_\eta=\gamma\psi(kp_2\times\gamma+ki_2\times\dot{\gamma}) \tag{21}$$

kp_2 and ki_2 are feedback gains.

In PATTERN 2, one motor is used to drive the wheel, and the other two motors are utilized to drive link 2 or link 4 to emulate the torso and arms' movements in order to obtain longitudinal stability. By this method, the wheel's movement will cause loss of the longitudinal stability, but the other two motors will drive link 2 or link 4 according to the posture of the unicycle in the pitch direction due to the wheel's movement. Meanwhile, those two motors' mounted positions are changed with the wheel's movement; this will make the motors for link 2 or link 4 highly coupled with the motor for the wheel. The unicycle's longitudinal stability is determined both by the wheel's movement and the movement of link 2 or link 4. As pointed out in section 2, the torque for link 2 is the same as that for link 4. The torque for the wheel and the torque for link 2 or link 4 are calculated in the following Eqs.(22) and (23). The torque for the turntable is the same as in Eq.(21).

Table 1 the unicycle parameters

m_w	m_b	m_1	m_2	m_4	e_1
1.0kg	3.5kg	0.5kg	0.5kg	2.0kg	0.43m
e_2	e_3	e_4	e_5	e_6	IWX
0.215m	0.12m	0.215m	0.33m	0.66m	0.014kg·m²
IWY	IWZ	IBX	IBY	IBZ	I1X
0.029kg·m²	0.014kg·m²	0.032kg·m²	0.033kg·m²	0.0012kg·m²	0kg·m²
I1Y	I1Z	I2X	I2Y	I2Z	ITX
0.0077kg·m²	0.0077kg·m²	0kg·m²	0.0077kg·m²	0.0077kg·m²	0.108kg·m²
ITY	ITZ	f_ψ	f_α	f_β	f_{θ_1}
0.108kg·m²	0.216kg·m²	0.25	0.25	0.15	0.15
f_{θ_3}	f_{θ_3}	f_{θ_4}	f_t	r_w	r_t
0.15	0.15	0.15	0.2	0.20m	0.4m

$$\tau_\psi=A\sin(2\pi\omega t) \tag{22}$$

$$\tau\theta_2=\tau\theta_4=-kp_1\times\beta-ki_1\times\dot{\beta} \tag{23}$$

τ_ψ is torque for the wheel; τ_{θ_2} and τ_{θ_4} are torques for link 2 and link 4 respectively. The meanings of other symbols is the same as in Eq.(20) and Eq.(21).

5. Computer Simulation Result

The unicycle parameters used in the computer simulation are shown in Table 1. The simulation is carried out by Runge-Kutta-Gill method. By PATTERN 1, the results with feedback gains kp_1=3000.0, ki_1=60.0, kp_2=1600.0, ki_2=50.0, A=10.0 and ω=1.0 are reported in Fig. 7. The simulation is conducted from the initial state with α=0.01 rad, β=0.01 rad and γ=0.01 rad. By PATTERN 2, the results with feedback gains kp_1=1500.0, ki_1=30.0, kp_2=1600.0, k_{i2}=50.0, A=10.0 and ω=1.0 are displayed in Fig. 8. The simulation is also executed from the initial state with α=0.01 rad, β=0.01 rad and γ=0.01 rad. Figure 7(a) indicates the change of longitudinal stability; the body's inclination in the pitch direction is always varied repeatedly in a small range according to the wheel's motion, and there exists a change like a limit cycle. Figures 7(b) and (c) demonstrate the lateral stability which can be attained quickly, and roll angle is controlled to zero within a short time, whereas the yaw angle does not return to zero for lateral stability. Figure 7(d) shows that the wheel's speed is affected by longitudinal stability. The torques τ_{θ_1} and τ_{θ_3} are shown in Fig. 7(e), where the required torque for longitudinal stability control is changed quickly according to the body's posture in the pitch direction. The torque shown in Fig. 7(f) is the torque for the turntable. After the lateral stability is obtained, the control on the turntable is not required, because the stability is maintained. The result shown in Fig. 8 is similar to Fig. 7. The body's inclination in the pitch direction is always changed repeatedly within a smaller range according to the wheel's motion, and the change is similar to a limit cycle, as illustrated in Fig. 8(a).

Figures 8(b) and (c) show the lateral stability, similar to Figs. 7(b) and (c); only the amplitude is different.

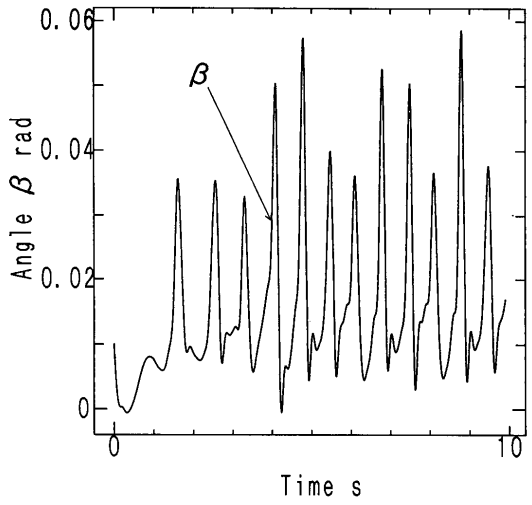

(a) Change of β with time

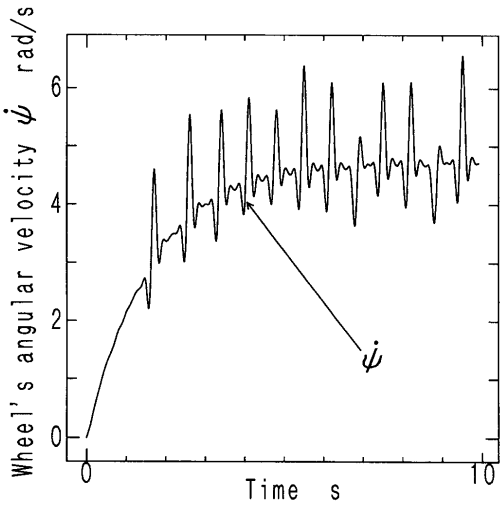

(d) Change of $\dot{\psi}$ with time

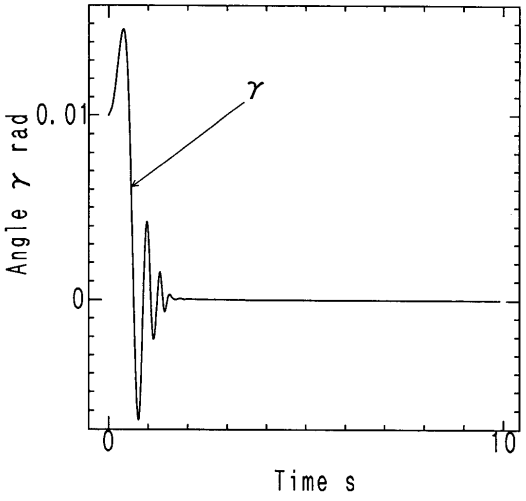

(b) Change of γ with time

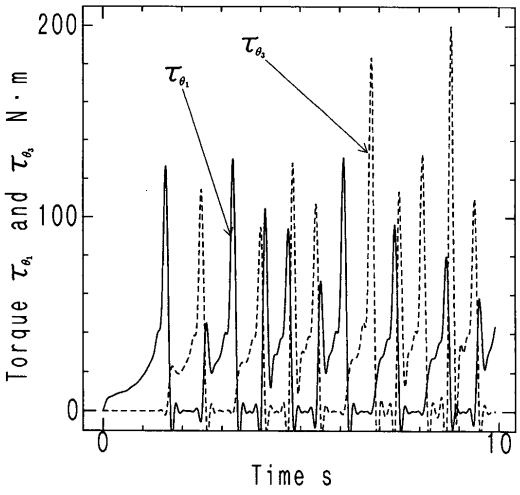

(e) Change of τ_{θ_1} and τ_{θ_2} with time

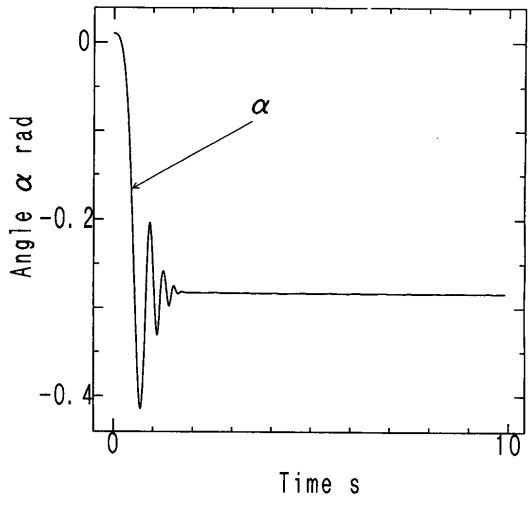

(c) Change of α with time

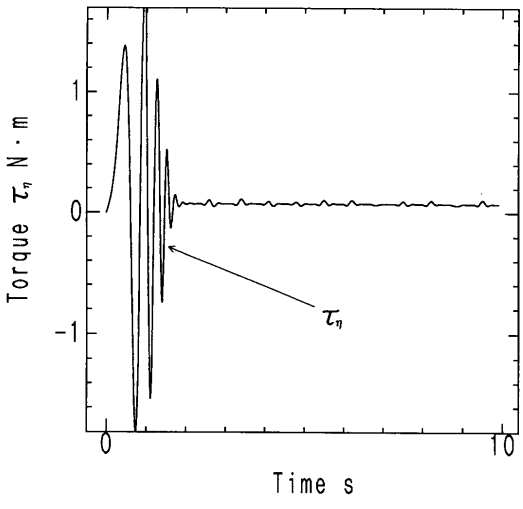

(f) Change of τ_η with time

Fig. 7 Simulation result by PATTERN 1

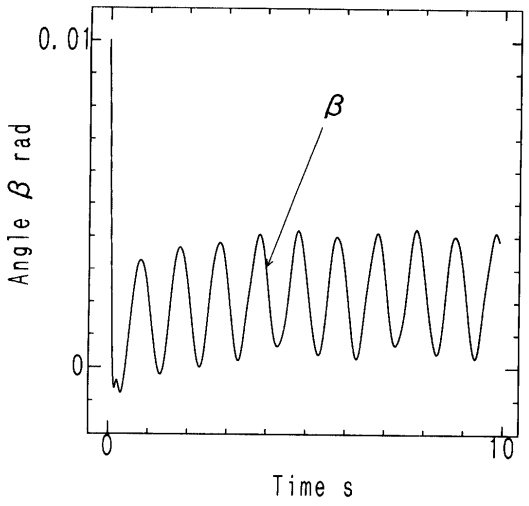

(a) Change of β with time

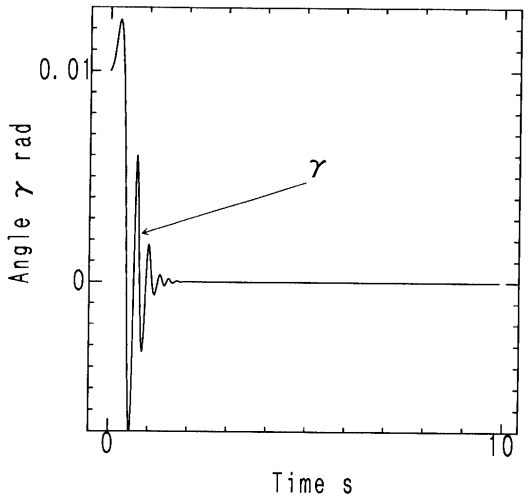

(b) Change of γ with time

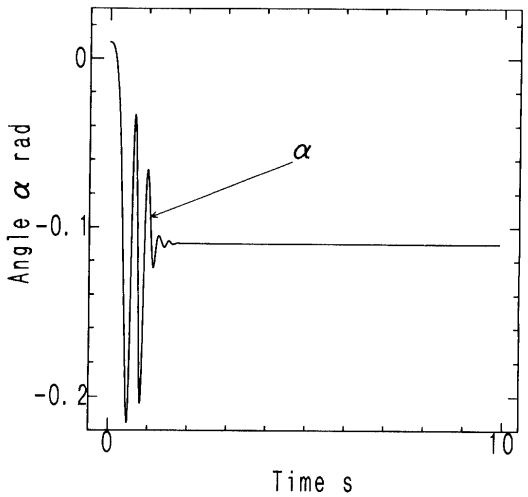

(c) Change of α with time

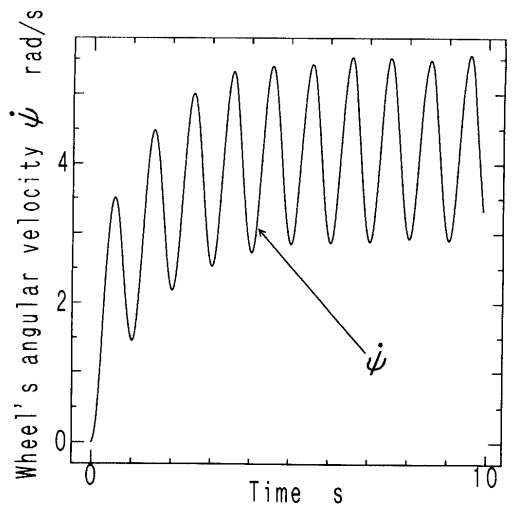

(d) Change of $\dot{\psi}$ with time

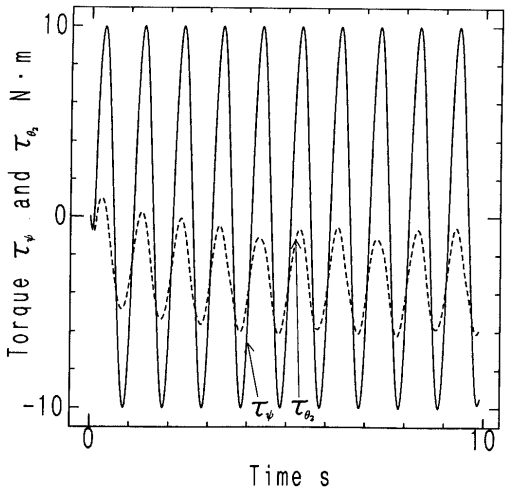

(e) Change of τ_ψ and τ_{θ_2} with time

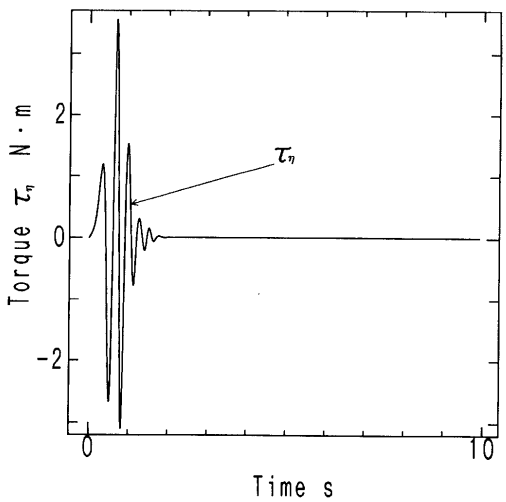

(f) Change of τ_η with time

Fig. 8 Simulation result by PATTERN 2

Figure 8(d) shows that the wheel's speed is affected by longitudinal stability, but the change in speed is not so sharp as shown in Fig. 7(d).

Figure 8(e) indicates that the torque for link 2 or link 4 is changed following the change in torque for the wheel at the same frequency, and the required torque is not as large as in Fig. 7(e). Figure 8(f) is also similar to Fig. 7(f).

Although the stability can be obtained by PATTERN 1 and with this pattern only two motors are required, the required torque is as large as in Fig. 8(e). Moreover, it is not practical to adopt this pattern. The reason for this kind of result is that the two motors are needed not only for driving the wheel but also for emulating the torso and arms' movement. Furthermore, as shown in Fig. 1, the rider inputs force both at joint 1 and joint 2 or joint 3 to drive the wheel, but in PATTERN 1, the force is applied only at joint A 1 or A 2. In this case, the robot cannot overcome the effect brought about by a singular joint existing in closed-link mechanisms.

In PATTERN 2, even though one more motor is required compared with PATTERN 1, and the closed-link mechanisms become redundant structures because of this added motor, the torque requirement is not as strict or large as in PATTERN 1. The reason is that in this pattern the wheel drive is realized by one actuator, and the emulation of the torso and arms' movement is realized by another actuator. Considering the symmetry and practicality of design, the second actuator is divided into two identical actuators at joints C and F, as shown in Fig. 2. Furthermore, the actuator for the wheel and the actuator for link 2 or link 4 are highly coupled through the two closed-link mechanisms, and it is by this method that the closed-link mechanism plays an important role in the unicycle's stability. In short, PATTERN 2 is more practical and close to the actual human riding a unicycle.

6. Conclusions

In this study, we investigated the unicycle stability problem by observing a human riding a unicycle, modeling it by a robot, and conducting simulations on it. The conclusions can be summarized as follows.

(1) From the observation and analysis of the human riding a unicycle, we found that the rider's body, thighs, and shanks, and the pedals on unicycle form a special structure with two closed-link mechanisms. We are convinced that this special structure plays an important role in the human-riding-unicycle system. Based on this idea, a new model for emulating the unicycle by robot is proposed.

(2) The unicycle's motion is not only constrained by nonholonomic constraints due to the rolling motion between wheel and ground, but it also has two closed-link mechanisms in its structure. Considering all of these special features, we have developed dynamic equations of motion for this new model.

(3) The computer simulation was carried out by using the Runge-Kutta-Gill method under the proposed control algorithms. The result implies that this new model is valid, and well represents a human riding a unicycle.

References

(1) Takanishi, A., Ishida, M., Yamazaki, Y. and Kato, I., The Realization of Dynamic Walking by the Biped Walking Robot WL-10 RD, Proc. of Int. Conf. on Advanced Robotics, (1985), p. 459.

(2) Raibert, Marc. H., Cheppon, M. and Brown, H. B., Jr., Running on Four Legs As Though They Were One, IEEE J. of Robotics and Automation, Vol. RA-2, No. 2 (1986), p. 70.

(3) Sano, A. and Furusho, J., Dynamically Stable Quadruped Locomotion (A Pace Gait in the COLT-3), Proc. of Int. Symp. on Industrial Robots, (1989), p. 253.

(4) Feng, Q. and Yamafuji, K., Design and Simulation of Control System of an Inverted Pendulum, Robotica, 6-3 (1988), p. 235.

(5) Yamafuji, K. and Inoue, K., Study on the Postural Stability of a Unicycle, JSME/JSPE Symp. in Yamanashi, Japan, (in Japanese), (1986), p. 4.

(6) Schoonwinkel, A., Design and Test of a Computer Stabilized Unicycle, Ph. D. Thesis, Stanford University, (1987).

(7) Vos, David W. and von Flotow, Andreas H., Dynamics and Nonlinear Adaptive Control of an Autonomous Unicycle (Theory and Experiment), Proc. of 29th Conf. on Decision and Control, (1990), p. 182.

(8) Borah, I., Young, L.R. and Curry, R.E., Sensory Mechanism Modeling, Air Force Human Resources Laboratory Report, AFHRLTR-77-70, October 1977.

(9) Ormsby, C.C and Young, L.R., Integration of Semicircular Canal and Otolith Information for Multisensory Orientation Stimuli, Mathematical Biosciences, Vol. 34 (1977), p. 1.

(10) Sheng, Z. and Yamafuji, K., A General Method for the Direct Dynamic Computation of Closed Link Mechanisms, Journal of Robotics and Mechatronics, 6-2 (1994), p. 169.

(11) Rosenberg, R.M., Analytical Dynamics of Discrete Systems, (1977), Plenum Press.

(12) Yamafuji, K., Takemura, Y. and Fujimoto, H., Dynamic Walking Control of the One-legged Robot which has the Controlling Rotor, Trans. Jpn. Soc. Mech. Eng., Vol. 57, No. 538, C (1991), p. 1930.